Signed Distance Fields: A Natural Representation for Both Mapping and Planning

Signed Distance Fields: A Natural Representation for Both Mapping and Planning

Helen Oleynikova, Alex Millane, Zachary Taylor, Enric Galceran, Juan Nieto and Roland Siegwart
Autonomous Systems Lab, ETH Zürich

***Abstract*—How to represent a map of the environment is a key question of robotics. In this paper, we focus on suggesting a representation well-suited for online map building from vision-based data and online planning in 3D. We propose to combine a commonly-used representation in computer graphics and surface reconstruction, projective Truncated Signed Distance Field (TSDF), with a representation frequently used for collision checking and collision costs in planning, Euclidean Signed Distance Field (ESDF), and validate this combined approach in simulation. We argue that this type of map is better-suited for robotic applications than existing representations.**

I. Introduction

Any discussion of map representations in robotics generally has two sides: the perception side, which often focuses on creating high-quality 3D reconstructions of natural environments from limited sensor data, and the planning side, which uses pre-built maps to navigate through the environment in a safe and collision-free manner.

Mapping and planning often have very different requirements from an environmental representation. For mapping from the perception standpoint, it is often most important to be able to output a high-quality colored surface model, such as a mesh. For navigation and planning, it is often most essential to have fast collision checking and be able to compute clearance and direction toward nearest obstacles.

In this work, we focus on the intersection of these two fields, with special attention given to image-based sensing, such as stereo vision and RGB-D cameras: creating 3D maps, online, from noisy sensor data in order to be used by online planners for obstacle avoidance.

Euclidean Signed Distance Fields (ESDFs) have long been used in planning literature for collision checking (especially of complex shapes), inferring distances and gradients to objects for planning, and finding large free areas [1].

On the other hand, with the advent of RGB-D cameras, KinectFusion has brought projective Truncated Signed Distance Fields (TSDFs) into the forefront as a fast, flexible map representation that implicitly computes the position of the surface using zero crossings [2].

Though both of these representations are signed distance fields (SDFs), the way that the distance of a voxel is computed differs. In the case of the ESDFs, a free voxel's distance represents the Euclidean distance *to the nearest occupied voxel* (and vice-versa in the case of occupied voxels). The ESDF is computed for every voxel in the map. On the other hand, the distance of a voxel in a projective TSDF represents the distance to the surface *along the ray direction from the center of the sensor*, and is truncated to only have values very near the surface, allowing for greater compression and decreasing errors due to this approximate distance metric.

In this paper, we argue that these two approaches can be combined into one – and rather than computing separate representations for map building and planning, find a compromise that allows the same representation to be used for both.

We seek to evaluate the accuracy of ray-distance calculations versus Euclidean distance calculations given different numbers of viewpoints from a realistic vision-based sensor. We first remove the truncation requirement of the TSDF, and then evaluate how the ray distances compare to true Euclidean distances for planning purposes, and propose a hybrid approach that should retain the better qualities of both TSDFs and ESDFs for both mapping and planning.

We also offer some comparison to the most-used map representation for online 3D map building and planning in unstructured environments: Octomap [3].

The advantages of our proposed approach over map representations typically used for online planning are as follows:

- Allows a single map representation that's both well-suited for online construction from sensor data *and* usage for online planning.
- Has a more natural representation of object surface (zero-crossing of distance field), which allows easier and more accurate modeling of sensor noise.
- Separates sensor measurement (distance to surface) from measurement uncertainty (voxel weight).
- Allows fast look-up of occupancies of complex shapes, especially when represented as sets of spheres, for online planning.
- For optimization-based planning algorithms, has a natural gradient magnitude and direction both inside and outside obstacles – allowing trajectories to be 'pushed' out of collision using optimization.
- Allows extracting accurate meshed surface models for other applications.
- If desired, the same map can also be used for SLAM or state estimation, or can be built up de-coupled based on input from other state estimators.

We will cover the points in the following sections. First we will describe existing methods in both the mapping and planning fields, then discuss the advantages of using an SDF-based representation over an occupancy-based representation

The research leading to these results has received funding from the European Communitys Seventh Framework Programme (FP7) under grant-agreement n.608849 (EuRoC) and n.644128, (AEROWORKS).

like Octomap, and finally provide validation for the claim that the distances used in these two representations are comparable using simulation.

II. Related Work

This section discusses relevant previous work and details of the approaches in mapping and planning literature.

A. Mapping Literature

SDFs have long been used for representing 3D volumes in computer graphics [4] [5]. They have also been used to build offline reconstructions of objects from real sensor data since the 1990s [6].

However, TSDFs have come back into the forefront of computer vision and robotics in 2011 with the new RGB-D Kinect sensors and the work from Newcombe *et al.* on KinectFusion [2]. Their approach focuses on doing high-resolution, accurate 3D reconstructions from RGB-D data on a GPU in real-time, using a TSDF as the main representation. They provide a Simultaneous Localization and Mapping (SLAM) approach, which estimates the pose of the camera at the same time as creating the reconstruction.

There have been a number of extensions to this approach, including Kintinuous, which allows scanning much larger spaces [7], and FastFusion which allows online reconstruction on the CPU rather than GPU [8] in an octree-style voxel grid. The main end-result of these is to generate a high-fidelity mesh, usually using a marching cubes algorithm [9].

Another competing representation for high-resolution online mapping from RGB-D data is RGB-D SLAM [10], which uses surfels (small planar units with size, color, and surface normal) to represent 3D structure, as a volumetric analogue to sparse pointclouds. Such representations are able to take advantages of the SLAM techniques developed for sparse keypoint-based maps and are better suited to distorting geometry, for example in ElasticFusion [11] where the map is distorted when encountering loop closures. These methods generally have high accuracy for state estimation and high-quality models. However, Bylow *et al.* have shown that it is possible to have the same level of accuracy from TSDF-based maps [12].

Therefore, SDF-based representations are well-studied, fast, and accurate for online surface reconstruction. In the following section, we will discuss how SDF-based representations are used for planning.

B. Planning Literature

Maps are essential to planning collision-free paths, with the representation of the map defining both the quality of the resulting path, and also what kind of planning algorithms can be used.

The minimum amount of information a map must provide is occupancy of a given point in space. Assuming a fixed-size grid, this enables the use of many different classes of planning algorithm: search-based methods like A* and D*-Lite [13], sampling-based methods like RRTs [14].

Occupancy grids represent the most commonly-used type of map representation for planning in 2D [15]. The approach of Elfes *et al.* is to use a fixed-size grid, probabilistic model of sensor measurements and model observed (known) and unknown space explicitly, allowing the incorporation of complex sensor models and reasoning about the environment. There are now many options available off-the-shelf that will run a complete 2D SLAM system online and provide occupancy grids of previously unknown environments [16], and countless planning algorithms that take 2D occupancy grids as input [17].

Naively extending occupancy grids to 3D, however, leads to huge memory requirements as well as slow ray-casts and look-ups for any space larger than a room. The solution most commonly used in 3D contexts while building a map online is Octomap [3]. This approach uses an octree-based representation of occupancy probabilities of cells in 3D space. The octree structure allows large blocks of space with the same probability to be represented by a single large cell, therefore vastly decreasing the amount of memory needed to represent areas of unknown or free space.

However, there are planning approaches which require additional information from a map. For example, trajectory optimization-based planners, such as CHOMP [1] and TrajOpt [18] require the distance to obstacles and occupancy gradient information. Algorithms such as these require an ESDF that is not truncated, and contains distance values over the entire voxel space. Usually these are constructed from another map representation, and often from a map hand-crafted out of object primitives (spheres, cubes) or high-fidelity mesh models of objects for manipulation [19].

Having a distance map also speeds up collision checking of complex shapes – for example, many-jointed robot arms are commonly represented as a set of overlapping spheres and check the distance field in the center of each sphere (which is one look-up in the ESDF per sphere) [20] [1] [21].

For gradient-based trajectory optimization methods, the collision cost (which is necessary to produce collision-free trajectories) also needs a gradient. For these, the ESDF gives a natural cost (a function, such as hinge loss [18] or a smoothed hinge loss [1] of the distance) and checking the distance values of the neighbors gives the gradient at a given point. This allows CHOMP and other such methods to follow the upward gradient of the distance to push points on the trajectory out of collision.

Wanger *et al* [22] is the closest work to our proposed approach, where a complete ESDF is built from the output of KinectFusion [2] and used for trajectory planning with CHOMP. However, their approach builds the entire ESDF at once from TSDF data, while our work focuses on exploring ways to combine these two representations into one.

In summary, SDFs allow for faster collision checking than occupancy grids while providing additional data needed for optimization-based planning methods.

III. SDF Advantages over Octomap

In this section, we make arguments about why using an SDF is a better map representation for both perception (creating the map) and planning (using the map for collision avoidance

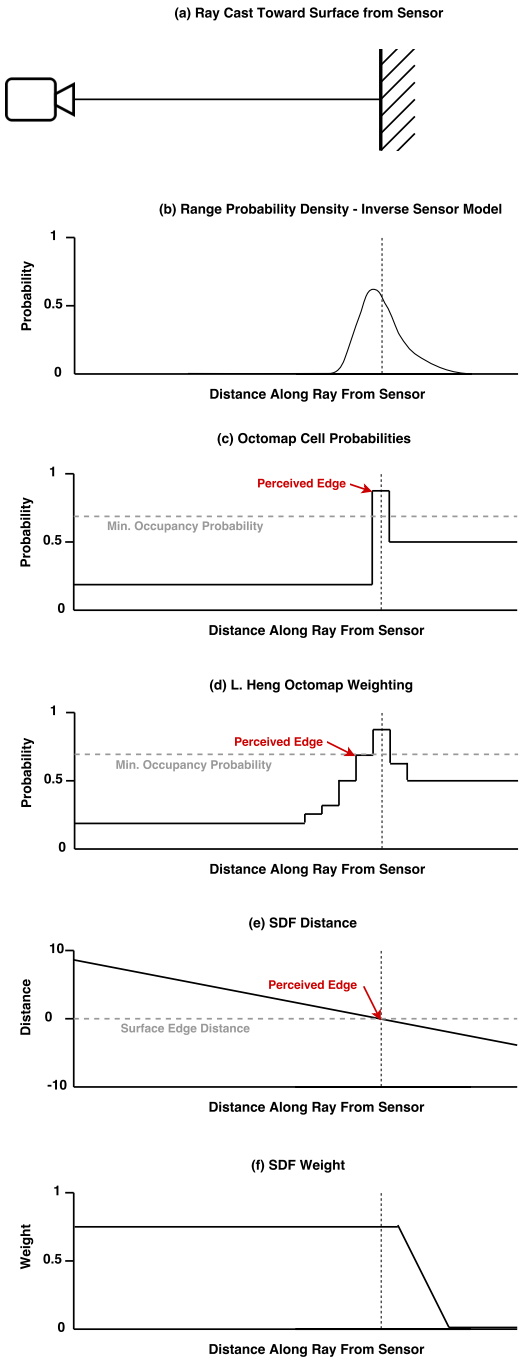

Fig. 1: Comparison of results from a single ray-cast in the various representations discussed: (a) diagram of a single vision-based sensor ray hitting a surface, (b) probability for range from an inverted stereo sensor model [23], (c) vanilla Octomap [3] probabilities of the raycast, (d) L. Heng Weighing [24], (e) TSDF (truncation radius not shown) [2], and (f) the TSDF weights along this ray [12]. Note that these are illustrations, and not to scale.

and clearance calculations) than the most commonly used 3D representation, the Octomap [3].

Since its advent, Octomap has been very widely used for 3D robotics applications, most notably for UAVs [24], [25]. We believe that this is due to a number of factors: first and not least, the open-source implementation and associated ROS wrappers have made it a very easy off-the-shelf solution for many applications. Second, the 'probabilistic' nature of the representation (assigning probabilities to each raycast, merging multiple observations of the same scene together) make it a good representation for noisy sensor data, such as stereo matching or RGB-D sensors where 'speckles' are common. This adds a level of low-pass filtering even to sensors exhibiting non-Gaussian error models. The third is due to memory efficiency and speed: the flexible voxel size allows representing large areas, and with some straight-forward optimizations, it is possible to get the insertion time of a dense stereo scan at 320x240 down to approximately 10 ms, and performing collision checks (even for a large bounding box) in this space is also very fast [24].

However, this representation also has downsides. The first is that the probability model used does does not accurately represent the error model of vision-based depth sensing. Since Octomap was originally designed to use with laser measurements, the accuracy of which does not degrade with distance to the sensor, the Octomap sensor model has a single probability of occupancy for one voxel at the end of the ray-cast. However, this is not an accurate model for stereo- or other vision-based sensing, where it is possible to have an expected error of over a meter at high distances, depending on the camera setup [23]. Heng *et al* implement a more realistic sensor model using distance weighing in the Octomap, however this tends to have the effect of inflating obstacles in the map [26].

Fig. 1 shows a representation of the different weighing representations for a single 1D ray within Octomap, compared to a TSDF representation. Fig. 1a shows a diagram of a ray cast from a depth camera hitting a wall, Fig. 1b shows the inverse sensor model for a stereo camera observing that wall, and Fig. 1c-d show vanilla and L. Heng weighing for the sensor hit. Since Octomap has a discrete cut-off probability for considering space occupied, the figure shows why L. Heng weighting tends to distort or inflate object boundaries.

One advantage of the TSDF is that even when discretized, it models a continuous function, as shown in Fig. 1e. Therefore it is possible to recover the position of the surface at a precision above the minimum voxel size, allowing the use of larger voxels and therefore smaller maps in memory.

The other advantage over Octomap is that TSDF has two values for each voxel: the distance to the surface (along the ray from the camera) and the weight/probability of this measurement. This allows us to more accurately model the actual error of vision-based depth estimates, and when merging multiple measurements, leads to a maximum-likelihood estimate of the surface, since the surface is found as a zero crossing. Bylow *et al* evaluate different weighing functions for TSDFs [12], and we show the linear weighing used by KinectFusion in Fig. 1f. However, since this value is separate from the actual distance measurement, any model can be incorporated without necessarily inflating the surface.

While the advantages for perception are clear, an SDF-based implementation has advantages in terms of path planning as well. Here we discuss the advantages of an ESDF (using Euclidean distances to nearest occupied/unoccupied space) over a binary occupancy-based representation. We will discuss how we can combine the TSDF and ESDF in the following section.

As discussed in Section II-B, an ESDF allows fast collision checks for complex shapes, as long as they can be expressed as a set of overlapping spheres. It also permits using gradient-based methods, as it gives a smooth cost of collision, which decreases as an object approaches free space. This also allows computation of collision cost gradients, and therefore choosing directions which lead to decreasing costs.

IV. Combining ESDF and TSDF: Results

The main difference between the two representations, TSDF for mapping and ESDF for planning, is the way that distances are computed. Both are signed distance fields, as the names suggest, but the distance in each voxel represents a different quantity.

In the ESDF, the distance in each voxel is the Euclidean distance *to the nearest occupied cell* (or if inside an object, distance to the nearest free cell). In the TSDF, on the other hand, the distance is computed *along the sensor ray* – that is, it represents a distance to the nearest occupied cell not in Euclidean space, but along this one-dimensional ray extending from the sensor center.

Here we present models showing how different ray distances (TSDF) are versus Euclidean distances (ESDF) and how this affects the quality of the map for planning. We focus on evaluating the metrics that are important for planning, especially for local optimization-based planners: error in distance to obstacles and direction of the gradient of the field.

We suggest four strategies to evaluate. The first two are building a projecting TSDF without a minimum truncation distance with two different strategies for merging multiple scans into the map:

1. Average the sensor value with the map value, giving equal weight to both (average weighing)
2. Take the minimum distance outside obstacles, and the maximum distance inside (minimum weighing)

We also propose a hybrid E/TSDF, where outside some minimum truncation distance, we iteratively compute Euclidean distances based on the projective distances inside the truncation radius with every new integrated scan. Finally, we also present the 'standard' approach for comparison, where we compute an occupancy grid and calculate Euclidean distances from that grid after building the complete map.

We use a vastly simplified model of the TSDF in 2D and a simulated sensor with a 70° field of view, 0.5° angular resolution, and a maximum range of $8m$. There is no noise on this sensor, but it is discretized to the voxel size. The sample environment attempts to mimic an enclosed office space of $10m \times 10m$ with many occlusions, some geometric and some organic shapes. Fig. 2a shows the occupancy map we use for

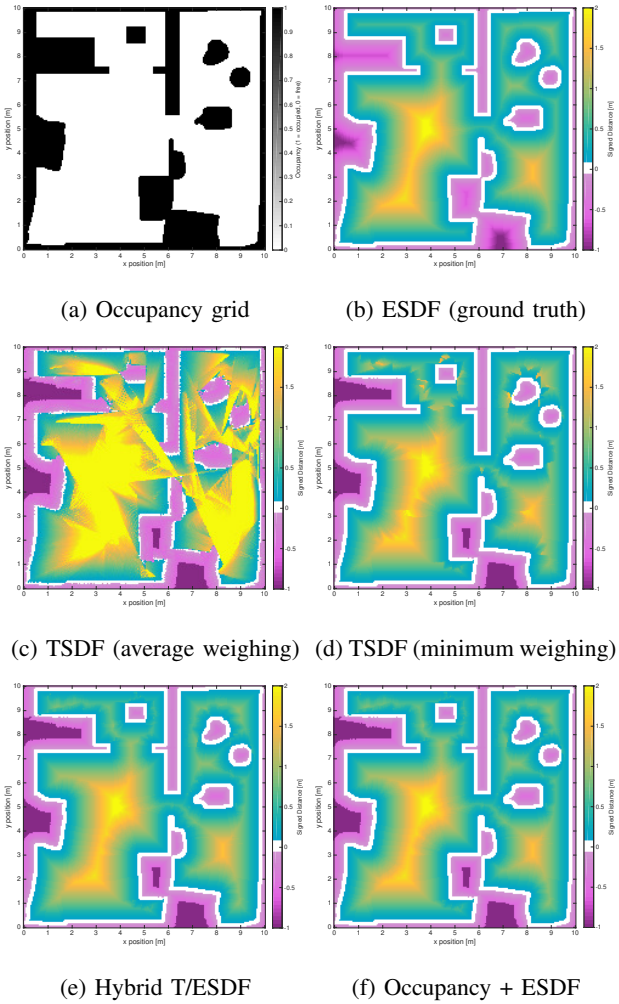

(a) Occupancy grid (b) ESDF (ground truth)

(c) TSDF (average weighing) (d) TSDF (minimum weighing)

(e) Hybrid T/ESDF (f) Occupancy + ESDF

Fig. 2: Results of various weighing schemes in SDF, using 500 viewpoints. White represents the observed surface of the object (zero crossings), green and yellow are areas outside the object, and pink are areas inside the object. Quantitative comparison is presented in Table I.

the simulations and Fig. 2b shows the ground-truth ESDF computed from this known map, where white is the object borders, pink is inside the objects, and green and yellow are distances (yellow being the furthest from an obstacle).

We generated random viewpoints within this space, sampling uniformly from unoccupied space and yaw. We then cast rays into this map, and generated distance measurements until $0.5m$ behind a surface. When raycasting into unknown space, the value was simply updated to the ray measurement value. When raycasting into space that has been observed before, we use the strategies described above.

Fig. 2c shows the TSDF generated with average weighing, and Fig. 2d shows the results of minimum weighing after 500 viewpoints. As can be seen, average weighing always overestimates the distance – as ray-distance is always greater than or equal to true Euclidean distance (it is equal in the

Viewpoints	TSDF Average Weighing		TSDF Min Weighing		Hybrid E/TSDF		Occupancy + ESDF		Unobserved Ratio
Mean Abs. Error $[m]$	r = $0.5m$	r = ∞	r = $0.5m$	r = ∞	r = $0.5m$	r = ∞	r = $0.5m$	r = ∞	
V = 10	0.699686	1.022263	0.501408	0.854449	**0.134561**	**0.480509**	0.162672	0.541797	0.659258
V = 50	0.730469	1.009407	0.317534	0.374416	**0.067819**	**0.078796**	0.070928	0.086687	0.054670
V = 100	0.717782	0.972221	0.157599	0.197076	0.042314	0.051344	**0.037105**	**0.049586**	0.010183
V = 500	0.628532	0.788858	0.031576	0.031498	0.015214	0.014252	**0.009491**	**0.010818**	0.000000
Gradient Error Mag. $[m]$	0.198165		0.014947		0.030057		**0.004643**		
Gradient Error Ang. $[^\circ]$	**6.065860**		8.699339		9.735610		8.699339		

TABLE I: Error analysis of different TSDF representations compared to ESDF. Results of the simulating a 2D SDF with a realistic sensor, comparing the error in using the TSDF distance (distance along the sensor ray) and comparing the error to the true ESDF (distance from nearest object). r is the radius around the surface at which errors are evaluated: $r = 0.5$ only evalutes distances close to the surface, while $r = \infty$ evaluates all distances in the map. Since below 500 viewpoints, not all parts of the map have been observed, we also give a Unobserved Ratio for reference.

case where the ray direction is along the surface normal, and greater in every other case). Whereas minimum weighing, over a large number of viewpoints, starts to converge to the true ESDF.

Of course, with fewer viewpoints, the estimate is worse – Table I shows the mean absolute error of distance measurements (taken only outside obstacles) over all observed voxels for different number of viewpoints. r is the radius around the surface at which errors are evaluated; $r = 0.5m$ is an estimate of the errors close to the surface, and $r = \infty$ is evaluated over the whole map. The values are compared to the ground-truth ESDF shown in Fig. 2b. However, this is not a strictly fair comparison, as all the viewpoint generated maps have discretization errors and not all obstacles are observed (for a lower number of viewpoints). We therefore also present the results for "Occupancy + ESDF", which was generated by creating a standard occupancy map from the sensor measurements and computing an ESDF from that map. It can be thought of as a lower bound on the error (though in some cases it actually has slightly higher error than other representations, which is due to discretization).

The other method we evaluate is a hybrid T/ESDF, which functions by behaving like a TSDF around surface edges, holding this surface section fixed and iteratively updating all other values using Euclidean distances. This retains the desirable quantities of both representations – near the surface for mapping and surface reconstruction, and further away from the surface for planning, while adding only slight computation cost per new viewpoint. Table I shows that this hybrid approach has the lowest errors of the TSDF-based approaches, and is comparable to the ESDF map built from occupancy grids.

This shows that depending on the weighing scheme, with sufficient distinct viewpoints, ray-distance approximates Euclidean distance, and there exist hybrid approaches that can further increase the accuracy of these combined maps.

V. Conclusions

In this paper, we compare two signed distance field representations: truncated signed distance fields (TSDFs), used for computer graphics and surface reconstruction from depth data, and Euclidean signed distance fields (ESDFs), used in planning for fast collision checking and cost and gradient information for optimization-based path planners.

We show the advantages of SDF-based maps for online map building and online planning in 3D compared to the commonly-used Octomap representation [3] and validate some of our claims by showing that projective ray-distances (used in TSDFs) can approximate Euclidean distances (used in ESDFs) when using sufficient viewpoints and an intelligent merging strategy. We also propose a hybrid approach which has advantages of both ESDFs and TSDFs.

We hope that this work can be a starting point for considering different map representations for online mapping for planning and navigation in 3D.

References

[1] M. Zucker, N. Ratliff, A. D. Dragan, M. Pivtoraiko, M. Klingensmith, C. M. Dellin, J. A. Bagnell, and S. S. Srinivasa, "Chomp: Covariant hamiltonian optimization for motion planning," *The International Journal of Robotics Research*, vol. 32, no. 9-10, pp. 1164–1193, 2013.

[2] R. A. Newcombe, S. Izadi, O. Hilliges, D. Molyneaux, D. Kim, A. J. Davison, P. Kohi, J. Shotton, S. Hodges, and A. Fitzgibbon, "Kinectfusion: Real-time dense surface mapping and tracking," in *Mixed and augmented reality (ISMAR), 2011 10th IEEE international symposium on*, pp. 127–136, IEEE, 2011.

[3] A. Hornung, K. M. Wurm, M. Bennewitz, C. Stachniss, and W. Burgard, "Octomap: An efficient probabilistic 3d mapping framework based on octrees," *Autonomous Robots*, vol. 34, no. 3, pp. 189–206, 2013.

[4] S. F. Gibson, "Using distance maps for accurate surface representation in sampled volumes," in *Volume Visualization, 1998. IEEE Symposium on*, pp. 23–30, IEEE, 1998.

[5] S. F. Frisken, R. N. Perry, A. P. Rockwood, and T. R. Jones, "Adaptively sampled distance fields: a general representation of shape for computer graphics," in *Proceedings of the 27th annual conference on Computer graphics and interactive techniques*, pp. 249–254, ACM Press/Addison-Wesley Publishing Co., 2000.

[6] B. Curless and M. Levoy, "A volumetric method for building complex models from range images," in *Proceedings of the 23rd annual conference on Computer graphics and interactive techniques*, pp. 303–312, ACM, 1996.

[7] T. Whelan, M. Kaess, M. Fallon, H. Johannsson, J. Leonard, and J. McDonald, "Kintinuous: Spatially extended kinectfusion," in *RSS Workshop on RGB-D: Advanced Reasoning with Depth Cameras*, 2012.

[8] F. Steinbrucker, J. Sturm, and D. Cremers, "Volumetric 3d mapping in real-time on a cpu," in *IEEE International Conference on Robotics and Automation (ICRA)*, pp. 2021–2028, IEEE, 2014.

[9] W. E. Lorensen and H. E. Cline, "Marching cubes: A high resolution 3d surface construction algorithm," in *ACM siggraph computer graphics*, vol. 21, pp. 163–169, ACM, 1987.

[10] P. Henry, M. Krainin, E. Herbst, X. Ren, and D. Fox, "Rgb-d mapping: Using kinect-style depth cameras for dense 3d modeling of indoor environments," *The International Journal of Robotics Research*, vol. 31, no. 5, pp. 647–663, 2012.

[11] T. Whelan, S. Leutenegger, R. F. Salas-Moreno, B. Glocker, and A. J. Davison, "Elasticfusion: Dense slam without a pose graph," in *Proceedings of Robotics: Science and Systems (RSS)*, 2015.

[12] E. Bylow, J. Sturm, C. Kerl, F. Kahl, and D. Cremers, "Real-time camera tracking and 3d reconstruction using signed distance functions," in *Robotics: Science and Systems (RSS) Conference 2013*, vol. 9, Robotics: Science and Systems, 2013.

[13] S. Koenig and M. Likhachev, "Fast replanning for navigation in unknown terrain," *Robotics, IEEE Transactions on*, vol. 21, no. 3, pp. 354–363, 2005.

[14] S. M. LaValle and J. J. Kuffner, "Randomized kinodynamic planning," *The International Journal of Robotics Research*, vol. 20, no. 5, pp. 378–400, 2001.

[15] A. Elfes, "Using occupancy grids for mobile robot perception and navigation," *Computer*, vol. 22, no. 6, pp. 46–57, 1989.

[16] J. Machado Santos, D. Portugal, and R. P. Rocha, "An evaluation of 2d slam techniques available in robot operating system," in *Safety, Security, and Rescue Robotics (SSRR), 2013 IEEE International Symposium on*, pp. 1–6, IEEE, 2013.

[17] D. Fox, W. Burgard, S. Thrun, and A. B. Cremers, "A hybrid collision avoidance method for mobile robots," in *Robotics and Automation, 1998. Proceedings. 1998 IEEE International Conference on*, vol. 2, pp. 1238–1243, IEEE, 1998.

[18] J. Schulman, Y. Duan, J. Ho, A. Lee, I. Awwal, H. Bradlow, J. Pan, S. Patil, K. Goldberg, and P. Abbeel, "Motion planning with sequential convex optimization and convex collision checking," *The International Journal of Robotics Research*, vol. 33, no. 9, pp. 1251–1270, 2014.

[19] J. Pan, S. Chitta, and D. Manocha, "Fcl: A general purpose library for collision and proximity queries," in *IEEE International Conference on Robotics and Automation (ICRA)*, pp. 3859–3866, IEEE, 2012.

[20] Q.-Z. Ye, "The signed euclidean distance transform and its applications," in *Pattern Recognition, 1988., 9th International Conference on*, pp. 495–499, IEEE, 1988.

[21] M. Kalakrishnan, S. Chitta, E. Theodorou, P. Pastor, and S. Schaal, "Stomp: Stochastic trajectory optimization for motion planning," in *IEEE International Conference on Robotics and Automation (ICRA)*, pp. 4569–4574, IEEE, 2011.

[22] R. Wagner, U. Frese, and B. Bauml, "3d modeling, distance and gradient computation for motion planning: A direct gpgpu approach," in *IEEE International Conference on Robotics and Automation (ICRA)*, pp. 3586–3592, IEEE, 2013.

[23] C. Hernández, G. Vogiatzis, and R. Cipolla, "Probabilistic visibility for multi-view stereo," in *Computer Vision and Pattern Recognition, 2007. CVPR'07. IEEE Conference on*, pp. 1–8, IEEE, 2007.

[24] L. Heng, D. Honegger, G. H. Lee, L. Meier, P. Tanskanen, F. Fraundorfer, and M. Pollefeys, "Autonomous visual mapping and exploration with a micro aerial vehicle," *Journal of Field Robotics*, vol. 31, no. 4, pp. 654–675, 2014.

[25] M. Burri, H. Oleynikova, , M. W. Achtelik, and R. Siegwart, "Real-time visual-inertial mapping, re-localization and planning onboard mavs in unknown environments," in *IEEE/RSJ International Conference on Intelligent Robots and Systems (IROS)*, Sept 2015.

[26] L. Heng, L. Meier, P. Tanskanen, F. Fraundorfer, and M. Pollefeys, "Autonomous obstacle avoidance and maneuvering on a vision-guided mav using on-board processing," in *IEEE International Conference on Robotics and Automation (ICRA)*, pp. 2472–2477, IEEE, 2011.